

UDC 539.3

SELECTION OF THE OPTIMAL DESIGN FOR A VIBRO-IMPACT NONLINEAR ENERGY SINK

P.P. Lizunov**O.S. Pogorelova****T.G. Postnikova**

*Kyiv National University of Construction and Architecture
31, Povitroflotskyave., Kyiv, Ukraine, 03680*

DOI: 10.32347/2410-2547.2023.111.13-24

The efficiency of a vibro-impact nonlinear energy sink (VI NES), that is, a vibro-impact damper, is largely determined by its design. The optimal damper design can be found through optimization procedures. However, the result of their work is ambiguous, their various options show different values of the optimal damper parameters. A thorough analysis of the obtained parameters values allow you to select the best option according to a certain criterion. While carrying out this analysis, we observe many interesting phenomena, namely, the synergistic effect of multiple parameters, rich complex dynamics of the VI NES, the presence of direct impacts between the damper and the main body, the dependence of the total energy on the exciting force parameters. The analysis also allows us to formulate the limitations of the VI NES. All these problems are reflected in this article.

Keywords: vibro-impact, primary structure, damper, nonlinear energy sink, synergistic effect.

1. Introduction

Different vibration control devices have received close attention from scientists and engineers over the years. Passive, active and hybrid control systems have been developed. Passive control devices and systems are commonly less complex and do not rely on a constant source of power, so they are often used. In particular, a tuned mass damper (TMD) is a traditional and popular mechanical vibrational absorber that is often implemented in high-rise buildings and towers [1,2]. In recent decades, the world scientific literature discusses fairly new passive vibration control device – nonlinear energy sink – NES [3,4]. A damper of small mass is coupled with the main body – the primary structure – by essentially nonlinear connection. This is its principal difference from TMD, where this connection is linear. However, a NES needs to be tuned like a TMD, that is, its parameters should be selected in such a way as to ensure the best mitigation of the primary structure vibrations. Modern computers and software make it possible to analyze the dynamic behavior of nonlinear systems and observe many nonlinear phenomena. So, we can study the motion of the system “primary structure – NES” with different dampers and choose an optimal NES design.

In modern world scientific literature, many works describe analytical, numerical and experimental investigations of NES. It is believed that these devices will be used to attenuate vibrations, in particular, in high-rise buildings and towers under the action of impulse, wind and even seismic loads. Numerous works on this topic demonstrate the active development of NES researches in recent years. There are comprehensive reviews of state-of-the-art researches on NESs [5-8], monographs [9,10], dissertations [4,11] and many articles on this problem [12-15]. Various types of NESs with the nonlinear connections of different types are studied. The restoring forces generated by these bonds may be smooth and non-smooth; they are discontinuous for vibro-impact NES – VI NES. A damper of this NES type repeatedly hits one or two constraints; the restoring force is discontinuous due these impacts; the “primary structure – NES” system is strongly nonlinear. The dynamic behavior of strongly nonlinear system is very sensitive to both the initial conditions and the parameters of the external load and the system itself. Therefore, the damper parameters need to be optimized in order to choose the optimal damper design to ensure its most effective operation [16]. Perhaps, the optimization mechanisms are not the same for different excitations. The author [11] emphasizes that a

feasible and precise design of VI NES to control vibrations of nonlinear systems will be difficult, despite the fact that preliminary experimental results demonstrate good reduction of velocity and, therefore, the effectiveness of energy reduction. The “impact rule” accepted in this investigation, that is, the impact simulation with nonlinear Hertz’s contact force according to his quasi-static contact theory makes it possible to optimize also the elastic properties of the contacting surfaces using Young’s moduli of elasticity and Poisson’s ratios.

In this paper, we continue the study of the SSVI NES dynamic behavior, started in our previous papers [17-20]. We analyze the feasibility of choosing the optimal damper design using various optimization procedures. Different optimization procedures show different results, which should be carefully checked and analyzed; the best option should be chosen among them. Since the optimization procedures do not give an univocal answer, choosing the optimal design becomes quite complex and requires a selection criterion. All options proposed by the optimization procedures clearly demonstrate the limitations of the VI NES. When considering the results of optimization procedures, the synergistic effect of multiple parameters is observed. Optimizing several damper parameters instead of two improves the damper efficiency and “calms” its complex dynamics, providing regular periodic motions instead of irregular regimes.

Thus, the goals of this paper are:

- compare the results of various optimization procedures and select the best among them according to a certain criterion;
- show the dynamics of VI NES with an optimal design;
- show the limitations of VI NES;
- demonstrate the synergistic effect of multiple parameters optimization.

2. Brief model description

Since this article continues the studies of VI NES, which were begun in our previous works [17-20], the mathematical model of the vibro-impact system under consideration was described in details in these works. Therefore, we will give its brief description that is necessary for understanding this text. The calculation scheme of two-body 2-DOF vibro-impact system (Fig.1) corresponds to the conceptual scheme of single-sided vibro-impact nonlinear energy sink (SSVI NES) [4, 17].

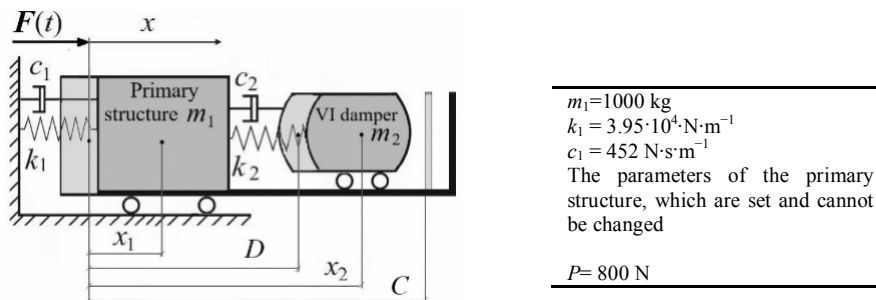


Fig. 1. Calculation scheme of SSVI NES

The damper mass m_2 should be much less than the primary structure mass m_1 , up to 1%. The connecting springs with stiffness k_1 and k_2 are linear. The base, along which the damper moves without friction, is rigidly connected to the primary structure and has a barrier at its right end. The nonlinearity and discontinuity of this system are created by the damper impacts on an obstacle and, as studies have shown, by the presence of collisions between bodies. The initial distance between the bodies is equal to D ; the distance to the right movable wall is C ; their difference defines the clearance, which is $(C-D)$.

The motion equations for this system are as follows:

$$\begin{aligned} m_1 \ddot{x}_1 + c_1 \dot{x}_1 + k_1 x_1 - c_2 (\dot{x}_2 - \dot{x}_1) - k_2 (x_2 - x_1 - D) &= F(t) - H(z) F_{con}(z) + H(z_1) F_{con}(z_1), \\ m_2 \ddot{x}_2 + c_2 (\dot{x}_2 - \dot{x}_1) + k_2 (x_2 - x_1 - D) &= +H(z) F_{con}(z) - H(z_1) F_{con}(z_1). \end{aligned} \quad (1)$$

The initial conditions are: at $t=0$ we have

$$x_1(0) = 0, x_2(0) = D, \dot{x}_1(0) = 0, \dot{x}_2(0) = 0, \varphi_0 = 0. \quad (2)$$

The exciting force is harmonic $F(t) = P \cos(\omega t + \varphi_0)$ with period $T = 2\pi/\omega$. In the future, we plan to study the dynamic behavior of the SSVI NES under action of impulsive, in particular, blast force. $H(z)$ is the Heaviside step function, which “actuates” the impact contact force $F(z)$ that acts only during an impact. It is this force that simulates an impact. We consider it as nonlinear and write it in accordance with Hertz’s contact quasi-static theory [21]. Since the damper hits both the primary structure directly and an obstacle, the contact forces are different for these impacts. The contact force at impact between the bodies has the following form:

$$F_{con}(z) = K[z(t)]^{3/2}, \quad K = \frac{4}{3} \frac{q}{(\delta_1 + \delta_2)\sqrt{A+B}}, \quad \delta_1 = \frac{1 - \nu_1^2}{E_1 \pi}, \quad \delta_2 = \frac{1 - \nu_2^2}{E_2 \pi}. \quad (3)$$

The contact force at impact on the right obstacle has the same form:

$$F_{con}(z_1) = K_1[z_1(t)]^{3/2}, \quad K_1 = \frac{4}{3} \frac{q_1}{(\delta_3 + \delta_4)\sqrt{A_1+B_1}}, \quad \delta_3 = \frac{1 - \nu_3^2}{E_3 \pi}, \quad \delta_4 = \frac{1 - \nu_4^2}{E_4 \pi}. \quad (4)$$

Here $\nu_1, \nu_2, \nu_3, \nu_4$ are Poisson’s ratios; E_1, E_2, E_3, E_4 are Young’s moduli of elasticity for fourth colliding surfaces; A, A_1, B, B_1, q, q_1 are constants characterizing the contact zones geometry. The absorber surfaces, both left and right, are assumed to be spherical with large radii R and R_1 (for example, $R=R_1=1$ m); the contact surfaces of the primary structure and the right obstacle are flat. Then $A=B=1/2R$, $A_1=B_1=1/2R_1$ ($A=A_1=B=B_1=0.5$ m⁻¹); $q=q_1=0.319$ as in the collision of a plane and a sphere. It is the moduli of elasticity and Poisson’s ratios that characterize the elastic properties of the colliding surfaces. Therefore, the analysis of their values should allow us to see the influence on the system dynamics in more detail than the analysis of the restitution coefficient. The variables z and z_1 are the colliding bodies rapprochement upon impact, since the Hertz’s theory allows local deformations in the contact zone.

A direct damper impact on the primary structure occurs when $x_1 \geq x_2$; $z = x_1 - x_2$. A damper impact on an obstacle occurs when $x_2 = x_1 + C$; $z_1 = x_2 - x_1 - C$.

3. Results and discussion

3.1. First version of the optimization procedure

The scientific literature recommends fulfilling the optimization procedures to provide such NES design that will ensure its maximum efficiency in mitigation of the primary structure vibrations. Our computational experience confirms the importance of this recommendation [Наши статті]. However, the optimization procedures performed in different ways produce different results, which need to be analyzed in order to choose the best one among them.

We carried out the optimization procedures in two versions using the *fmincon* and *fminsearch* programs of the *MatLab* platform and compared their results. In both versions, the optimization was performed in three stages. At the first stage, three or two damper parameters were optimized. In the second and third stages, four or five more parameters were optimized, so a total of 7 parameters were optimized.

In the first version of the optimization procedure, at the first stage three parameters were optimized: the damper mass m_2 , its stiffness k_2 , and the distance to the obstacle C , which

determines the clearance. In the second and third stages, the damping coefficient c_2 , the initial distance between the primary structure and the damper D , and Young's moduli of elasticity for the colliding surfaces E_2 and E_4 were optimized. They are shown in burgundy in the second rows in (5). In this way, the following two complete sets parameters were defined for two damper variants:

$$m_2=22.68 \text{ kg}, k_2=2481 \text{ N}\cdot\text{m}^{-1}, C=0.0683 \text{ m},$$

$$c_2=41.4 \text{ N}\cdot\text{s}\cdot\text{m}^{-1}, D=0.046 \text{ m}, E_2=2.26\cdot 10^7 \text{ N}\cdot\text{m}^{-2}, E_4=2.18\cdot 10^7 \text{ N}\cdot\text{m}^{-2},$$

$$m_2=37.88 \text{ kg}, k_2=414.6 \text{ N}\cdot\text{m}^{-1}, C=0.0747 \text{ m}, \tag{5}$$

$$c_2=27.9 \text{ N}\cdot\text{s}\cdot\text{m}^{-1}, D=0.057 \text{ m}, E_2=2.21\cdot 10^7 \text{ N}\cdot\text{m}^{-2}, E_4=2.05\cdot 10^7 \text{ N}\cdot\text{m}^{-2}.$$

The comparison of the dynamic behavior of the vibro-impact system with the dampers with 3 and 7 optimized parameters demonstrates the synergistic effect of the multiple parameters. The damper efficiency changes little, but the dynamic behavior is completely different. Table 1 shows this difference depending on the exciting force frequency.

Table 1

Regimes implemented in a system with dampers with different numbers of optimized parameters depending on the exciting force frequency at $P=800 \text{ N}$

$\omega, \text{rad}\cdot\text{s}^{-1}$	6.2	6.3	6.4	6.5	6.7	7.0
$m_2=22.7 \text{ kg}$						
with 3 optimized parameters	Chaotic	Chaotic; Intermittency	Chaotic; intermittency	Chaotic; intermittency	$T,1,2$	$T,0,2$
with 7 optimized parameters	Chaotic	Chaotic	4 $T,8, 8$	$T,1,2$	$T,1,2$	$T,1,2$
$m_2=37.9 \text{ kg}$						
with 3 optimized parameters	Intermittency	Chaotic	Chaotic	Chaotic	$T,2,2$	Chaotic
with 7 optimized parameters	Transient chaos; $T,3,3$	Chaotic	Transient chaos; $T,2,3$	Chaotic	Transient chaos; $T,2,2$	Chaotic

Following the logic of [22], we use the notation nT,k,m , which defines the regime of periodicity nT (where T is the exciting force period) with k impacts between the damper and the primary structure and m impacts of the damper on an obstacle. The Table clearly shows a rich complex dynamics that is realized in a vibro-impact system consisting of a primary structure coupled to a NES. Indeed, in [8], the authors note this phenomenon as one of the VI NES disadvantages: "One disadvantage of VI NESs is that coupling it with a primary structures leads to very complex nonlinear dynamics that is difficult to analyze analytically without making several simplifications". The Table also shows the presence of the direct damper impacts on the primary structure in all realized modes.

Fig. 2 and Fig. 3 show the characteristics of the complex modes that occur in a vibro-impact system with these two dampers with 7 optimized parameters at an exciting force frequency close to the resonant one $\omega=6.2 \text{ rad}\cdot\text{s}^{-1}$. The presence of direct impacts between the VI NES and the primary structure is very clearly visible.

Fig. 2 shows the picture that is typical for the chaotic movement. In particular, a ball of the phase trajectories in Fig. 2 (d) and a smear of the Poincaré map in Fig. 2 (b), (c) confirm its chaoticity. The contact forces in Fig. 2 (b) significantly exceed the exciting force. Fig. 2 (c) of

the relative damper displacements clearly shows the direct damper impacts on the primary structure at $(x_2-x_1) = 0$ and on an obstacle at $(x_2-x_1) = C = 0.0683$ m.

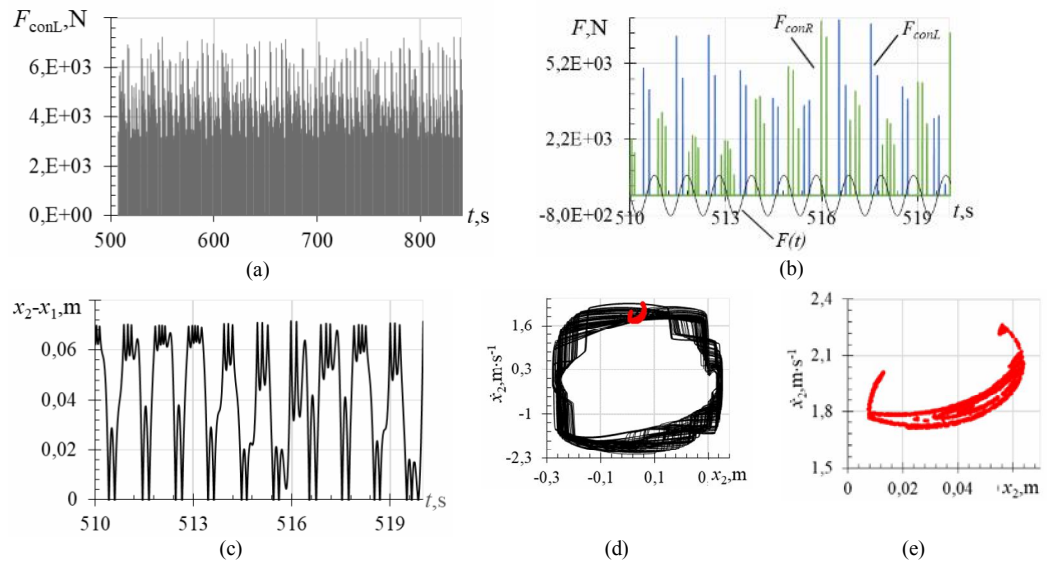


Fig. 2. The characteristics of chaotic regime for the system with a damper of mass $m_2=22.7$ kg with 7 optimized parameters at the exciting force frequency $\omega = 6.2$ rad·s⁻¹. (a) Contact forces during damper impacts on the primary structure directly. (b) Contact forces when the damper hits both the primary structure directly in blue and an obstacle in green over a narrower exciting force range. (c) The relative damper displacements. (d) Phase trajectories with Poincaré map in red for the damper. (e) The Poincaré map for the damper

Fig. 3 shows a typical form of transient chaos, when chaotic motion abruptly turns into the periodic one for the same values of all parameters. Fig. 3 presents the movement characteristics in both phases – in chaotic and in periodic $T_{3,3}$.

Fig.3 (c) on the right panel clearly shows 3 direct damper impacts on the primary structure at $(x_2-x_1) = 0$ and 3 damper impacts on an obstacle at $(x_2-x_1) = C = 0.0747$ m. The phase trajectory in the form of a closed curve and one point of the Poincaré map on the right panel in Fig. 3 (d) correspond to T -periodic motion. 6 jumps of damper velocity in this figure occur in 6 impacts per cycle - 3 on the primary structure and 3 on an obstacle.

3.2. Second version of the optimization procedure

The second version of the optimization procedure differs from the first version in the exciting force frequency for which the objective function was calculated. In the first version, this frequency was far from the resonant one $\omega=7.23$ rad·s⁻¹. On the contrary, in the second version it is almost resonant one $\omega=6.3$ rad·s⁻¹. At the first stage of the second optimization procedure version, two damper parameters were optimized: its mass m_2 and stiffness k_2 . The remaining five parameters were optimized in the second and third stages. The two complete sets of parameters for the two dampers are as follows:

$$m_2=39.67 \text{ kg}, k_2=1550.7 \text{ N}\cdot\text{m}^{-1},$$

$$C=0.1244 \text{ m}, c_2=643.6 \text{ N}\cdot\text{s}\cdot\text{m}^{-1}, D=0.1002 \text{ m}, E_2=2.205\cdot 10^7 \text{ N}\cdot\text{m}^{-2}, E_4=2.047\cdot 10^7 \text{ N}\cdot\text{m}^{-2},$$

$$m_2=62.02 \text{ kg}, k_2= 198.24 \text{ N}\cdot\text{m}^{-1},$$

$$C=0.0498 \text{ m}, c_2=538.8 \text{ N}\cdot\text{s}\cdot\text{m}^{-1}, D=0.000001 \text{ m}, E_2=2.205\cdot 10^7 \text{ N}\cdot\text{m}^{-2}, E_4=2.047\cdot 10^7 \text{ N}\cdot\text{m}^{-2}.$$

These parameters are very different from the previous ones. Firstly, the dampers masses m_2 are larger. The scientific literature recommends that the NES mass be of 1% of the primary structure mass. In the first version of the optimization procedure, the minimum damper mass was determined to be 2%, in the second version – 4 %. Secondly, the remaining parameters – the damper stiffness k_2 , the damping coefficient c_2 , the distances D and C , which define the

clearance, vary greatly even for close damper masses $m_2= 37.88$ kg and 39.67 kg. Here again, the dynamic behavior of a system with dampers with two and seven optimized parameters is also very different that demonstrates the synergistic effect of the multiple parameters. Table 2 demonstrates the manifestation of the synergistic effect in a strong change in the implemented motion regimes.

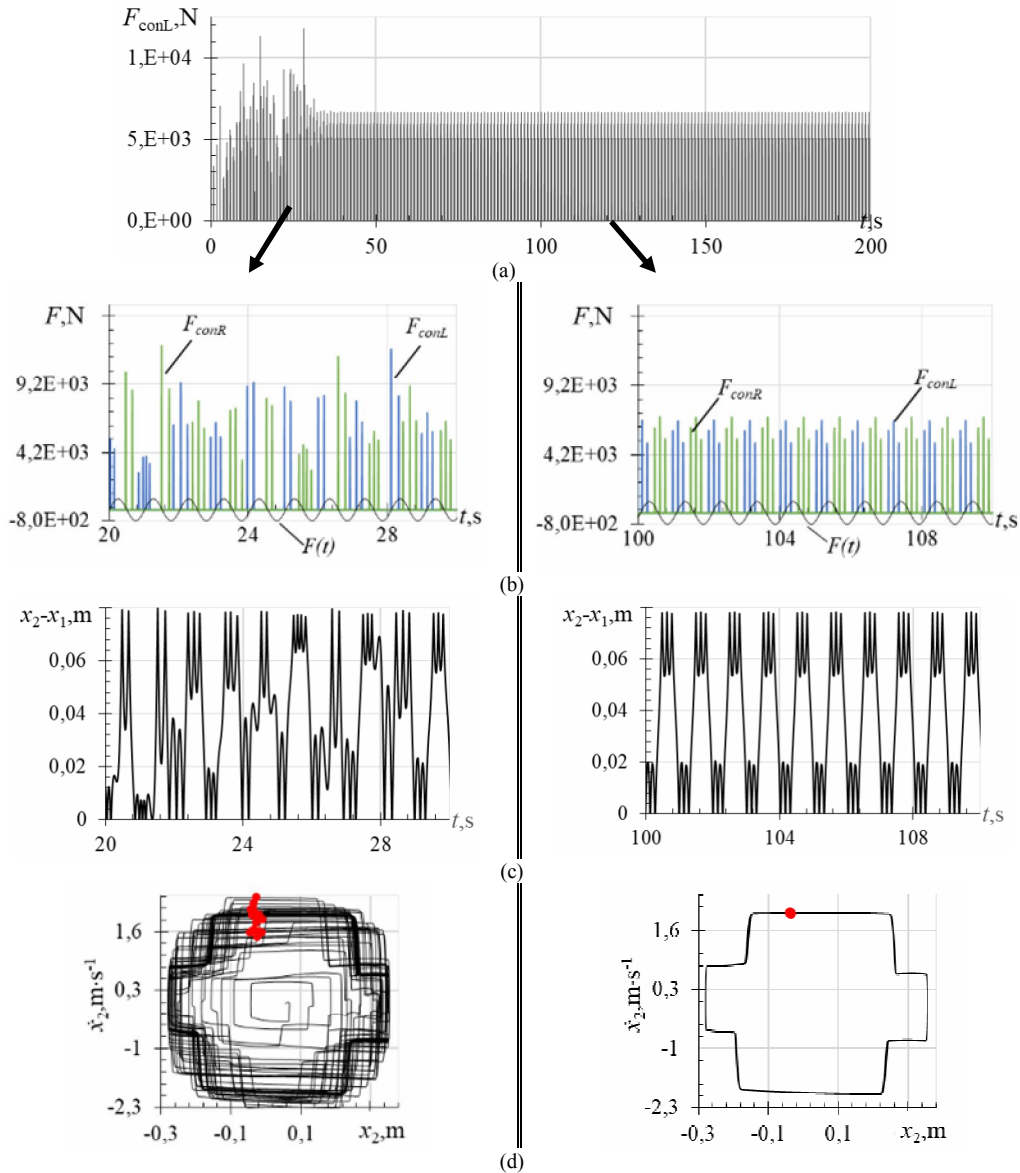


Fig. 3. The characteristics of transient chaos turning into periodic $T_{3,3}$ for the system with a damper of mass $m_2=37.9$ kg with 7 optimized parameters at the exciting force frequency $\omega = 6.2 \text{ rad} \cdot \text{s}^{-1}$. (a) Contact forces during damper impacts on the primary structure directly. (b) Contact forces when the damper hits both the primary structure directly in blue and an obstacle in green over a narrower exciting force range. (c) The relative damper displacements. (d) Phase trajectories with Poincaré map in red for the damper

Table 2

Regimes implemented in a system with dampers with different numbers of optimized parameters depending on the exciting force frequency at $P=800$ N

$\omega, \text{rad}\cdot\text{s}^{-1}$	6.2	6.3	6.4	6.5	6.7	7.0
$m_2=39.7$ kg						
with 2 optimized parameters	T,3,3	Transient chaos; T,2,4	T,2,3	Chaotic	Chaotic	T,1,2
with 7 optimized parameters	T,1,2	T,1,2	T,0,2	T,0,1	T,0,1	T,0,1
$m_2=62.0$ kg						
with 2 optimized parameters	Chaotic	Chaotic	Chaotic	Transient chaos; T,2,2	Chaotic	Chaotic
with 7 optimized parameters	Chatter	T,3,3	Chatter	T,2,2	T,2,2	T,2,1

For these dampers with 7 optimized parameters, the system movement is “calmed down”; irregular modes are replaced by regular periodic regimes. For the damper $m_2=39.7$ kg, we see the modes without direct damper impacts on the primary structure. Thus, different optimization procedures produce different damper parameters, so analysis is necessary to define, which variant is the most effective.

3.3. Selecting the optimal damper parameters

A logical question arises: which of these four options, determined by the optimization procedures, is preferable? Which option provides the best damper performance?

Let us compare the efficiency of four damper variants with 7 optimized parameters, that is, let us see how they attenuate the primary structure energy.

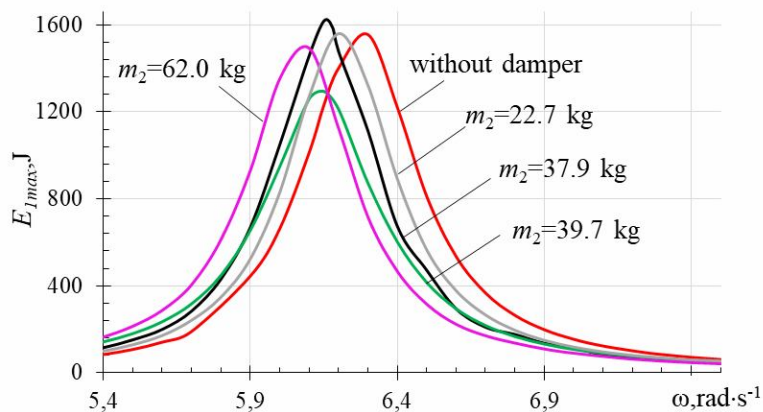


Fig. 4. The maximum total energy of the primary structure coupled with different SSVI NES depending on the exciting force frequency

Fig. 4 shows that all dampers shift the resonant peak of the maximum total energy of the primary structure to the left towards the low exciting force frequencies. Only a damper with a mass of $m_2=39.7$ kg (green curve) significantly reduces it; a damper with a mass of $m_2=62.0$ kg (lilac curve) reduces it a little. The energy mitigation occurs at fairly high frequencies. At low frequencies, the primary structure energy not only does not attenuate, but, on the contrary, increases. We believe that from these 4 variants proposed by the optimization procedures, it is worth choosing a damper of mass $m_2=39.7$ kg (green curve in Fig.4). Firstly, it reduces the energy resonant peak quite well, better than other dampers. Secondly, it attenuates the primary

structure energy at high frequencies also better than other dampers. Thirdly, it ensures regular periodic motion over a wide frequency range, as shown in Table 2. Its mass is 4% of the primary structure mass. It is worth noting that at high frequencies a damper with mass $m_2=62.0$ kg mitigates the energy better. However, it is too heavy (its mass has 6% of the primary structure mass) and provides a high resonant peak. Table 3 shows the attenuation of the maximum total energy of the primary structure coupled with the dampers of mass $m_2=39.7$ kg and mass $m_2=62.0$ kg.

Table 3

Attenuation of the maximum total energy of the primary structure coupled with the dampers of masses $m_2=39.7$ kg and $m_2=62.0$ kg, depending on the exciting force frequency

ω rad·s ⁻¹	6.2	6.3	6.4	6.5	6.7	7.0
$E_{1\max}$ wane % for $m_2=39.7$ kg	13.7	44.1	50.8	49.0	41.2	31.4
$E_{1\max}$ wane % for $m_2=62.0$ kg	20.1	54.2	61.9	61.4	53.9	42.5

As Table 2 shows, a vibro-impact system with damper of mass $m_2=39.7$ kg performs the regular periodic motion even without direct damper impacts on the primary structure at higher exciting force frequencies. Fig. 5 shows the movement characteristics of the $T_{1,2}$ regime at the same exciting force frequency $\omega = 6.2$ rad·s⁻¹.

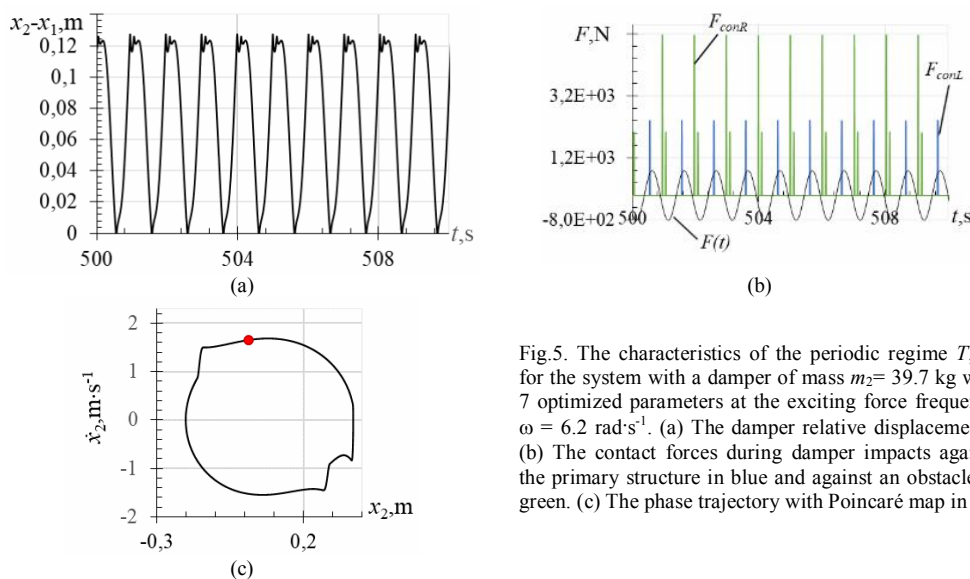


Fig.5. The characteristics of the periodic regime $T_{1,2}$ for the system with a damper of mass $m_2=39.7$ kg with 7 optimized parameters at the exciting force frequency $\omega = 6.2$ rad·s⁻¹. (a) The damper relative displacements. (b) The contact forces during damper impacts against the primary structure in blue and against an obstacle in green. (c) The phase trajectory with Poincaré map in red

The relative damper displacements in Fig. 5 (a) show one direct impact between the damper and the primary structure at $(x_2-x_1) = 0$ and two damper impacts on an obstacle at $(x_2-x_1) = C = 0.1224$ m. The contact forces graph in Fig. 5(b) shows one force per cycle when the damper directly impacts the primary structure in blue and two forces per cycle when the damper hits an obstacle in green. The exciting force is also shown in this graph. Fig. 5 (c) presents the phase trajectory with Poincaré map in red for a damper. This is a closed curve with one point of the Poincaré map, which is typical for T -periodic movement.

Table 2 shows that the vibro-impact system with a heavy damper of a mass $m_2=62.0$ kg also performs regular periodic motion, but at some exciting force frequencies the movement deviates somewhat from the periodic one and becomes a motion that can be called “chatter”. It is interesting to compare the types of its characteristics with both periodic and chaotic regimes. Fig. 6 demonstrates the characteristics of regime “chatter” for a system with the heavy damper

of mass $m_2=62.0$ kg with 7 optimized parameters at the same exciting force frequency $\omega = 6.2$ $\text{rad}\cdot\text{s}^{-1}$.

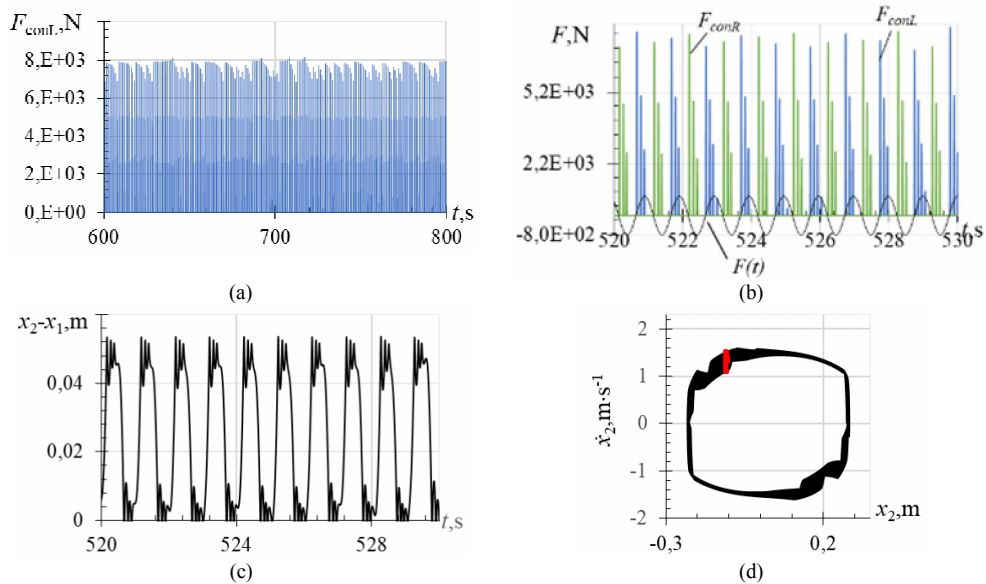


Fig. 6. The characteristics of “chatter” mode for the system with the damper of mass $m_2 = 62.0$ kg with 7 optimized parameters at the exciting force frequency $\omega = 6.2$ $\text{rad}\cdot\text{s}^{-1}$. (a) Contact forces during damper impacts on the primary structure directly. (b) Contact forces when the damper hits both the primary structure directly in blue and an obstacle in green over a narrower exciting force range. (c) The relative damper displacements. (d) Phase trajectories with Poincaré map in red for the damper

4. Conclusions

The research results described above allow us to draw the following conclusions.

- It is necessary to optimize the VI NES parameters in order to select such its design that will ensure the most efficient operation.
 - Different optimization procedures give different results, so the obtained values of the VI NES parameters must be carefully analyzed in order to choose those values that will ensure the most efficient operation.
 - It is necessary to pay attention to the synergistic effect of multiple parameters, so as many parameters as possible should be optimized.
 - A well-designed damper in combination with the primary structure shifts the resonant peak of its energy to the left towards low frequencies and reduces it. A damper mitigates the primary structure energy well at the exciting force frequencies above the resonant one. On the contrary, it not only does not attenuate its energy, but increases it at low exciting force frequencies lower than the resonant one.
 - The dynamics of a vibro-impact system “the primary structure – VI NES” is rich and complex. We see many different irregular regimes. However, the complex dynamics practically does not change the damper efficiency, because the oscillatory amplitudes and velocities of the heavy primary structure change little under these regimes, but the contact forces change strongly.
 - Direct impacts between the primary structure and the damper occur in almost all regimes. This means that the single-sided VI NES operates like a double-sided one, in which the primary structure itself is the second barrier.
- Summarizing, we want to highlight the limitations of VI NES. They do not attenuate the primary structure energy at the exciting force frequencies below the resonant one. The choice of its optimal design is complex and ambiguous.

REFERENCES

1. Gutierrez Soto M., Adeli H. Tuned mass dampers //Archives of Computational Methods in Engineering. – 2013. – T. 20. – C. 419-431.<https://doi.org/10.1007/s11831-013-9091-7>
2. Rahimi F., Aghayari R., Samali B. Application of tuned mass dampers for structural vibration control: a state-of-the-art review //Civil Engineering Journal. – 2020. – C. 1622-1651. <https://doi.org/10.28991/cej-2020-03091571>
3. Ding H., Chen L. Q. Designs, analysis, and applications of nonlinear energy sinks //Nonlinear Dynamics. – 2020. – T. 100. – №. 4. – C. 3061-3107.<https://doi.org/10.1007/s11071-020-05724-1>
4. Wierschem NE. Targeted energy transfer using nonlinear energy sinks for the attenuation of transient loads on building structures:PhD dissertation. University of Illinois at Urbana-Champaign (USA); 2014.<https://www.proquest.com/openview/31588e3789383c3132b6e1e5bd4de07b/1?cb1=18750&loginDisplay=true&pq-origsite=gscholar>
5. Vakakis A. F. Passive nonlinear targeted energy transfer //Philosophical Transactions of the Royal Society A: Mathematical, Physical and Engineering Sciences. – 2018. – T. 376. – №. 2127. – C. 20170132.<https://doi.org/10.1098/rsta.2017.0132>
6. Lu Z. et al. Particle impact dampers: Past, present, and future //Structural Control and Health Monitoring. – 2018. – T. 25. – №. 1. – C. e2058.<https://doi.org/10.1002/stc.2058>
7. Ibrahim R. A. Recent advances in nonlinear passive vibration isolators //Journal of sound and vibration. – 2008. – T. 314. – №. 3-5. – C. 371-452.<https://doi.org/10.1016/j.jsv.2008.01.014>
8. Saeed A. S., Abdul Nasar R., AL-Shudeifat M. A. A review on nonlinear energy sinks: designs, analysis and applications of impact and rotary types //Nonlinear Dynamics. – 2023. – T. 111. – №. 1. – C. 1-37.<https://doi.org/10.1007/s11071-022-08094-y>
9. Lee Y. S. et al. Passive non-linear targeted energy transfer and its applications to vibration absorption: a review //Proceedings of the Institution of Mechanical Engineers, Part K: Journal of Multi-body Dynamics. – 2008. – T. 222. – №. 2. – C. 77-134.<https://doi.org/10.1243/14644193jmbd118>
10. Wang J. et al. Track nonlinear energy sink for rapid response reduction in building structures //Journal of Engineering Mechanics. – 2015. – T. 141. – №. 1. – C. 04014104.[https://doi.org/10.1061/\(asce\)em.1943-7889.0000824](https://doi.org/10.1061/(asce)em.1943-7889.0000824)
11. Li T. Study of nonlinear targeted energy transfer by vibro-impact :PhD thesis. National Institute of Applied Sciences of Toulouse (France); 2016.<https://www.theses.fr/20161SAT0007>
12. Youssef B., Leine R. I. A complete set of design rules for a vibro-impact NES based on a multiple scales approximation of a nonlinear mode //Journal of Sound and Vibration. – 2021. – T. 501. – C. 116043.<https://doi.org/10.1016/j.jsv.2021.116043>
13. Bergeot B., Bellizzi S., Berger S. Dynamic behavior analysis of a mechanical system with two unstable modes coupled to a single nonlinear energy sink //Communications in Nonlinear Science and Numerical Simulation. – 2021. – T. 95. – C. 105623.<https://doi.org/10.1016/j.cnsns.2020.105623>
14. Saeed A. S. et al. Two-dimensional nonlinear energy sink for effective passive seismic mitigation //Communications in Nonlinear Science and Numerical Simulation. – 2021. – T. 99. – C. 105787.<https://doi.org/10.1016/j.cnsns.2021.105787>
15. Luo J. et al. Large-scale experimental evaluation and numerical simulation of a system of nonlinear energy sinks for seismic mitigation //Engineering Structures. – 2014. – T. 77. – C. 34-48.<https://doi.org/10.1016/j.engstruct.2014.07.020>
16. Wu Z., Seguy S., Paredes M. Basic constraints for design optimization of cubic and bistable nonlinear energy sink //Journal of Vibration and Acoustics. – 2022. – T. 144. – №. 2. – C. 021003.<https://doi.org/10.1115/1.4051548>
17. Lizunov P., Pogorelova O., Postnikova T. Choice of the Model for Vibro-impact Nonlinear Energy Sink //Strength of Materials and Theory of Structures. – 2022. – №. 108. – C. 63-76.<https://doi.org/10.32347/2410-2547.2022.108.63-76>
18. Lizunov P., Pogorelova O., Postnikova T. Dynamics of primary structure coupled with single-sided vibro-impact nonlinear energy sink //Strength of Materials and Theory of Structures. – 2022. – №. 109. – C. 20-29.<https://doi.org/10.32347/2410-2547.2022.109.20-29>
19. Lizunov P. P., Pogorelova O., Postnikova T. Vibro-impact damper dynamics depending on system parameters. – 2023. Research Square. <https://doi.org/10.21203/rs.3.rs-2786639/v1>
20. Lizunov P., Pogorelova O., Postnikova T. Influence of stiffness parameters on vibro-impact damper dynamics //Strength of Materials and Theory of Structures. – 2023. – №. 110. – C. 21-35.<https://doi.org/10.32347/2410-2547.2023.110.21-35>
21. Johnson KL. Contact Mechanics. Cambridge University Press; 1985. <https://doi.org/10.1017/cbo9781139171731>
22. Lamarque C. H., Janin O. Modal analysis of mechanical systems with impact non-linearities: limitations to a modal superposition //Journal of Sound and Vibration. – 2000. – T. 235. – №. 4. – C. 567-609.<https://doi.org/10.1006/jsvi.1999.2932>

Стаття надійшла 16.10.2023

Лізунов П.П., Погорелова О.С., Постнікова Т.Г.

ВИБІР ОПТИМАЛЬНОГО ДИЗАЙНУ ДЛЯ ВІБРО-УДАРНОГО НЕЛІНІЙНОГО ПОГЛИНАЧА ЕНЕРГІЇ

Ефективність віброударного нелінійного поглинача енергії (vibro-impact nonlinear energy sink - VINES), тобто вібро-ударного демпфера, значною мірою визначається його конструкцією. Оптимальний дизайн демпфера можна підібрати за допомогою процедур оптимізації. Однак результат їхньої роботи неоднозначний, їхні різні варіанти показують різні значення оптимальних параметрів демпфера. Ретельний аналіз отриманих значень параметрів дозволяє підібрати оптимальний варіант за певним критерієм. Проводячи цей аналіз, ми спостерігали багато цікавих явищ, а саме синергетичний ефект багатьох параметрів, багату комплексну динаміку VI NES, наявність прямих ударів між демпфером і головним тілом, залежність повної енергії від параметрів збуджуючої сили. Аналіз також дозволяє сформулювати обмеження VI NES. Всі ці проблеми відображені в цій статті.

Ключові слова: віброударний, первинна структура, демпфер, нелінійний поглинач енергії, синергетичний ефект.

Lizunov P.P., Pogorelova O.S., Postnikova T.G.

SELECTION OF THE OPTIMAL DESIGN FOR A VIBRO-IMPACT NONLINEAR ENERGY SINK

The efficiency of a vibro-impact nonlinear energy sink (VI NES), that is, a vibro-impact damper, is largely determined by its design. The optimal damper design can be found through optimization procedures. However, the result of their work is ambiguous, their various options show different values of the optimal damper parameters. A thorough analysis of the obtained parameters values allow you to select the best option according to a certain criterion. While carrying out this analysis, we observe many interesting phenomena, namely, the synergistic effect of multiple parameters, rich complex dynamics of the VI NES, the presence of direct impacts between the damper and the main body, the dependence of the total energy on the exciting force parameters. The analysis also allows us to formulate the limitations of the VI NES. All these problems are reflected in this article.

Keywords: vibro-impact, primary structure, damper, nonlinear energy sink, synergistic effect.

УДК 539.3

Лізунов П.П., Погорелова О.С., Постнікова Т.Г. **Вибір оптимального дизайну для вібро-ударного нелінійного поглинача енергії** // Опір матеріалів і теорія споруд: наук.-тех. збірн. – К.: КНУБА. 2023. – Вип. 111. – С. 13-24. – Англ.

Ефективність віброударного нелінійного поглинача енергії (vibro-impact nonlinear energy sink -VI NES), тобто вібро-ударного демпфера, значною мірою визначається його конструкцією. Оптимальний дизайн демпфера можна підібрати за допомогою процедур оптимізації. Однак результат їхньої роботи неоднозначний, їхні різні варіанти показують різні значення оптимальних параметрів демпфера. Ретельний аналіз отриманих значень параметрів дозволяє підібрати оптимальний варіант за певним критерієм. Проводячи цей аналіз, ми спостерігали багато цікавих явищ, а саме синергетичний ефект багатьох параметрів, багату комплексну динаміку VI NES, наявність прямих ударів між демпфером і головним тілом, залежність повної енергії від параметрів збуджуючої сили. Аналіз також дозволяє сформулювати обмеження VI NES. Всі ці проблеми відображені в цій статті.

Табл. 3. Рис. 6. Бібліогр. 22 назв.

UDC 539.3

Lizunov P.P., Pogorelova O.S., Postnikova T.G. **Selection of the optimal design for a vibro-impact nonlinear energy sink**//Strength of Materials and Theory of Structures: Scientific-and-technical collected articles. – К.: KNUBA. 2023. – Issue111. – P. 13-24.

The efficiency of a vibro-impact nonlinear energy sink (VI NES), that is, a vibro-impact damper, is largely determined by its design. The optimal damper design can be found through optimization procedures. However, the result of their work is ambiguous, their various options show different values of the optimal damper parameters. A thorough analysis of the obtained parameters values allow you to select the best option according to a certain criterion. While carrying out this analysis, we observe many interesting phenomena, namely, the synergistic effect of multiple parameters, rich complex dynamics of the VI NES, the presence of direct impacts between the damper and the main body, the dependence of the total energy on the exciting force parameters. The analysis also allows us to formulate the limitations of the VI NES. All these problems are reflected in this article.

Tabl. 3. Fig. 6. Ref. 22.

Автор (вчена ступень, вчене звання, посада): доктор технічних наук, професор, завідувач кафедри будівельної механіки КНУБА, директор НДІ будівельної механіки ЛІЗУНОВ Петро Петрович
Адреса: 03680 Україна, м. Київ, Повітрофлотський проспект 31, Київський національний університет будівництва і архітектури
Тел.: +38(044) 245-48-29
Мобільний тел.: +38(067)921-70-05
E-mail: lizunov@knuba.edu.ua
ORCID ID: <http://orcid.org/0000-0003-2924-3025>

Автор (вчена ступень, вчене звання, посада): кандидат фізико-математичних наук, старший науковий співробітник, провідний науковий співробітник НДІ будівельної механіки ПОГОРЕЛЮВА Ольга Семенівна
Адреса: 03680 Україна, м. Київ, Повітрофлотський проспект 31, Київський національний університет будівництва і архітектури
Тел.: +38(044) 245-48-29
Мобільний тел.: +38(067) 606-03-00
E-mail: pogos13@ukr.net
ORCID ID: <http://orcid.org/0000-0002-5522-3995>

Автор (вчена ступень, вчене звання, посада): кандидат технічних наук, старший науковий співробітник, старший науковий співробітник НДІ будівельної механіки ПОСТНІКОВА Тетяна Георгіївна
Адреса: 03680 Україна, м. Київ, Повітрофлотський проспект 31, Київський національний університет будівництва і архітектури
Тел.: +38(044) 245-48-29
Мобільний тел.: +38(050) 353-47-19
E-mail: postnikova.tg@knuba.edu.ua
ORCID ID: <https://orcid.org/0000-0002-6677-4127>